# COMPRESSIVE SPECTRAL IMAGING BASED ON COLORED CODED APERTURES

*Hoover Rueda*† *Henry Arguello*⋆ *Gonzalo R. Arce*†

† Department of Electrical and Computer Engineering, University of Delaware,
Newark, DE, 19716, USA
⋆ Universidad Industrial de Santander, Bucaramanga, Colombia
E-mail: {rueda, arce}@udel.edu, henarfu@uis.edu.co

## ABSTRACT

Compressive spectral imaging (CSI) systems capture the 3D spatio-spectral information of a scene by measuring 2D focal plane array (FPA) coded projections. A reconstruction algorithm exploiting the sparsity of the signal is then used to recover the underlying hyperspectral scene. CSI systems use a set of binary coded apertures, commonly realized through photomasks, to modulate the spatial characteristics of the scene. The reconstruction image quality in CSI is determined by the design of a 2D coded aperture binary set which block or unblock light from the scene onto the detector. This work extends the framework of CSI by replacing the traditional block-unblock photomasks by colored coded apertures which modulate the source not only spatially but spectrally as well. Simulations show a significant improvement in the quality of spectral image reconstructions.

***Index Terms***— Compressive sensing, patterned filters, hyperspectral imaging, coded apertures, optical imaging.

## 1. INTRODUCTION

Traditional spectral imaging sensors scan adjacent zones of a scene and merge the results to construct a spectral data cube. Push-broom spectral imaging sensors, for instance, capture a spectral data cube with one FPA measurement per spatial line of the scene [1]. Spectrometers based on optical band-pass filters need to scan the scene by tuning the band-pass filters in steps [2]. The disadvantage of these techniques is that they require scanning a number of zones that grows linearly in proportion to the desired spatial or spectral resolution. In contrast, compressive spectral imaging (CSI) senses 2D coded projections of the underlying scene such that the number of measurements is far less than that of traditional sensors. CSI exploits the fact that the representation of hyperspectral images is sparse in some basis. The Coded Aperture Snapshot Spectral Imager (CASSI) is a CSI sensor that attains compressive measurements [3, 4].

This research was supported in part by ONR under the contract NOOO14-1O-C-0 199 and by NSF under the grant CCF-0915800.

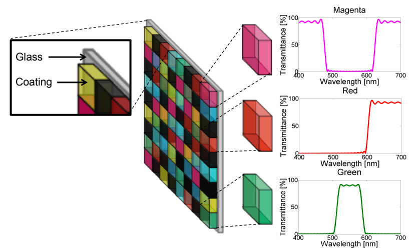


(a) Colored coded aperture design.

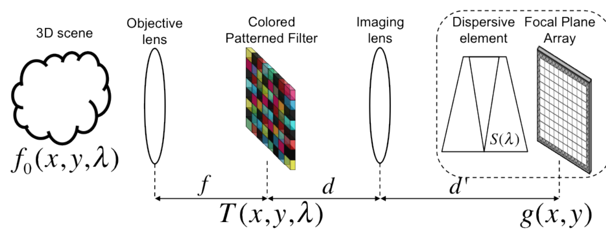


(b) Colored-CASSI.

**Fig. 1**: (a) Sketch of a colored coded aperture and (b) Color coded aperture-based CASSI system.

Coded apertures in CASSI have been fabricated using materials such as chrome-on-quartz [5] rendering coded aperture elements that are either opaque or transparent to the whole wavelengths of interest. These coded aperture masks are referred to as photomasks or "block-unblock" coded apertures. New advances in micro-lithography and coating technology have allowed the design of patterned optical coatings which are used to create multi-patterned arrays of different optical filters. Indeed, coatings can be designed with high resolution patterns which are used on multispectral sensors [6], micro-electro-mechanical devices [7, 8], optical waveguide-based devices, and gratings. Color-patterned coded apertures have been recently used in applications such as artificial compound eyes [9], multi-focusing and depth estimation [10], deblurring and matting [11]. This work incorporates colored coded apertures into compressive spectral imaging architectures, such that traditional photomask-based coded apertures are replaced by multi-patterned arrays of selectable optical filters (a.k.a. colored coded apertures). Figure 1 illustrates a sketch of a colored coded aperture and the proposed optical architecture. The colored coded aperture entries can be realizations of either low-pass($\mathcal{L}$), high-pass($\mathcal{H}$), band-pass($\mathcal{B}$), or blocking coatings. In the following sections, it is detailed the photomask-based optical spectral imaging model and that of compressive spectral imaging systems based on colored coded apertures. The signal reconstruction problem is analyzed for the new imaging system as well.

## 2. SYSTEM MODEL

### 2.1. Photomask-Based CASSI Model

The CASSI optical architecture is composed by five optical elements: an objective lens that focuses the scene onto the coded aperture image plane which modulates the amplitude of the incoming scene; an imaging lens which relays the coded field onto a dispersive element that disperses the light before it impinges onto the FPA detector. Denote the spatio-spectral power source density as $f_0(x, y, \lambda)$ where $x$ and $y$ index the spatial domain and $\lambda$ indexes the wavelength. The source density is first spatially modulated by the coded aperture $T(x, y)$, resulting in a coded field represented as, $f_1(x, y, \lambda) = T(x, y)f_0(x, y, \lambda)$. Subsequently, the coded field is dispersed by the dispersive element, whose output can be expressed as $f_2(x, y, \lambda) = \iint f_1(x', y', \lambda) \times h(x-x'-S(\lambda), y-y')dx'dy'$, where $h(x - x' - S(\lambda), y - y')$ is the optical impulse response of the system, and $S(\lambda)$ represents the dispersion, which occurs only in the horizontal direction. The spectral density just in front of the detector can be expressed as, $g(x, y) = \int f_2(x, y, \lambda)d\lambda$. Replacing the value of $f_2(x, y, \lambda)$, the signal measurement $g(x, y)$ is given by

$$\begin{aligned} g(x, y) = \iiint & T(x', y')f_0(x', y', \lambda) \\ & \times h(x - x' - S(\lambda), y - y')dx'dy'd\lambda. \end{aligned} \quad (1)$$

If the optical impulse response of the system is assumed linear, (1) can be succinctly expressed as

$$g(x, y) = \int T(x + S(\lambda), y)f_0(x + S(\lambda), y, \lambda)d\lambda. \quad (2)$$

Denoting the coded aperture pixel size as $\Delta_c$ the transmittance function of the coded aperture is given by

$$T(x, y) = \sum_{i,j} T_{i,j}\text{rect}\left(\frac{x}{\Delta_c} - i, \frac{y}{\Delta_c} - j\right), \quad (3)$$

where $T_{i,j}$ is a binary value accounting for the block $(0)$ or unblock $(1)$ operation at the $(i, j)^{th}$ spatial pixel, and rect$(\cdot)$ represents the rectangular step function. Besides, assuming the pixel size of the detector is $\Delta_d$, the effect of the integration of the continuous field $g(x, y)$ in a single $(n, m)^{th}$ detector pixel can be expressed as

$$G_{n,m} = \iint g(x, y)\text{rect}\left(\frac{x}{\Delta_d} - m, \frac{y}{\Delta_d} - n\right) dxdy. \quad (4)$$

Replacing Eqs. (2) and (3) in (4) lead to

$$\begin{aligned} G_{n,m} = \Bigg[ \iiint & \sum_{i,j} T_{i,j}\text{rect}\left(\frac{x + S(\lambda)}{\Delta_c} - i, \frac{y}{\Delta_c} - j\right) \\ \times \quad & \text{rect}\left(\frac{x}{\Delta_d} - m, \frac{y}{\Delta_d} - n\right) \\ \times \quad & f_0(x + S(\lambda), y, \lambda)d\lambda dxdy\Bigg] + \omega_{n,m} \end{aligned} \quad (5)$$

where $\omega_{n,m}$ accounts for the noise of the capturing process. Representing the spatio-spectral source density being integrated on the detector in discrete form as $F_{i,j,k}$, such that $i \in \{1, \ldots, N\}$ indexes the $x$-axis, $j \in \{1, \ldots, N\}$ the $y$-axis and $k \in \{1, \ldots, L\}$ the wavelength, Eq. (5) can be succinctly expressed as

$$G_{n,m} = \sum_k T_{n,m-k}F_{n,m-k,k} + \omega_{n,m} \quad (6)$$

for $n = 1, \ldots, N$, $m = 1, \ldots, N + L - 1$, where $N$ is the number of rows and $N + L - 1$ is the number of columns in the detector.

### 2.2. CASSI Model with Colored Coded Apertures

In the proposed approach, the photomask is replaced by a colored coded aperture, which modulates the source along the spectral and spatial coordinates. The colored coded aperture can be thus classified as a 3D coded aperture (Fig. 2). The CASSI system architecture with colored coded aperture is depicted in Fig. 1(b), where the traditional block-unblock photomask was replaced by the colored patterned filter presented in Fig. 1(a). The coding is now realized by the patterned filter denoted by $T(x, y, \lambda)$ as applied to the spatio-spectral density source $f_0(x, y, \lambda)$, resulting in the coded field $f_1(x, y, \lambda)$. This coded field differs from the one obtained with a photomask in that a single feature of the patterned filter permits to pass a desired set of wavelengths instead of blocking the complete spectrum at a given spatial location, as depicted in Fig. 2. In consequence, the energy in front of the FPA is now given by

$$g(x, y) = \int T(x + S(\lambda), y, \lambda)f_0(x + S(\lambda), y, \lambda)d\lambda, \quad (7)$$

where again the PSF of the system is assumed linear. Notice that, in contrast with Eq. (2), the colored coded aperture is represented in Eq. (7) as a three-dimensional optical element, accounting for the wavelength-dependency of the filters. Furthermore, it is represented by

$$T(x, y, \lambda) = \sum_{i,j,k} T_{i,j,k}\text{rect}\left(\frac{x}{\Delta_c} - i, \frac{y}{\Delta_c} - j, \frac{\lambda}{\Delta_d} - k\right), \quad (8)$$

where $T_{i,j,k}$ is a binary value accounting for the block-unblock operation at the $(i, j, k)^{th}$ voxel of the 3D coding

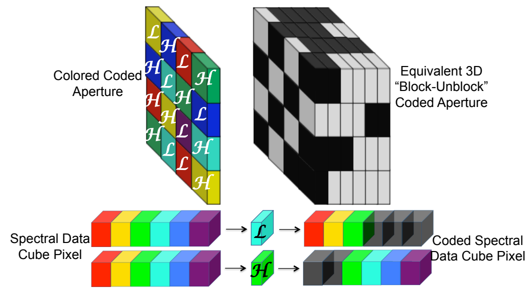


**Fig. 2**: 3D-coding performed by the colored-coded aperture. The colored coded aperture entries can be realizations of either low-pass($\mathcal{L}$) or high-pass($\mathcal{H}$) optical filters.

presented in Fig. 2. Accordingly, the FPA measurement based on the color-patterned filter can be written as

$$G_{n,m} = \sum_{k} T_{n,m-k,k} F_{n,m-k,k} + \omega_{n,m}. \tag{9}$$

Note that $T_{i,j}$ and $T_{i,j,k} \in \{0,1\}$ represent the entries of the photomask and the colored coded aperture, respectively. The ratio between the number of ones and the total of elements is defined as the transmittance $Tr$, and it is given by, $Tr = \sum_{i,j} \frac{T_{ij}}{N^2} \cdot 100$, for the photomask case and $Tr = \sum_{i,j,k} \frac{T_{ijk}}{N^2 L} \cdot 100$, for coloring coded apertures.

## 3. IMAGE RECONSTRUCTION

### 3.1. Colored Codes in CASSI Matrix Model

A projection in CASSI can be expressed in matrix form as $\mathbf{y} = \mathbf{H}\boldsymbol{f}$, where $\mathbf{H}$ is an $N(N+L-1) \times (N \cdot N \cdot L)$ matrix whose structure is determined by the photomask/colored coded aperture entries and the dispersive element effect, and $\boldsymbol{f}$ is the hyperspectral image in vector form. Here, $N \times N$ represents the spatial dimensions and $L$ is the spectral depth of the image cube. The CASSI architecture can be slightly modified to admit multiple snapshots, each one exhibiting a different coded aperture pattern. Multi-shot CASSI yield to a less ill-posed inverse problem and consequently improved signal recovering [5, 12, 13]. Particularly, denoting the $\ell^{th}$ FPA measurement as $\mathbf{y}^{\ell} = \mathbf{H}^{\ell}\boldsymbol{f}$, where $\mathbf{H}^{\ell}$ represents the effects of the $\ell^{th}$ photomask/colored coded aperture, the set of $K$ FPA measurements is then assembled as $\mathbf{y} = \left[(\mathbf{y}^0)^T, \ldots, (\mathbf{y}^{K-1})^T\right]^T$.

### 3.2. Reconstruction Algorithm

CSI supposes that the hyperspectral signal $\boldsymbol{\mathcal{F}} \in \mathbb{R}^{N \times N \times L}$, or its vector representation $\boldsymbol{f} \in \mathbb{R}^{N \cdot N \cdot L}$, is $S$-sparse on some basis $\boldsymbol{\Psi}$, such that $\boldsymbol{f} = \boldsymbol{\Psi}\boldsymbol{\theta}$ can be approximated by a linear combination of $S$ vectors from $\boldsymbol{\Psi}$ with $S \ll (N \cdot N \cdot L)$. Consequently, the projections in CASSI can be alternatively expressed as $\mathbf{y} = \mathbf{H}\boldsymbol{\Psi}\boldsymbol{\theta} = \mathbf{A}\boldsymbol{\theta}$ where the matrix $\mathbf{A} = \mathbf{H}\boldsymbol{\Psi}$ is the sensing matrix. Based on this assumption, CSI allows $\boldsymbol{f}$ to be recovered from $m$ random projections with high probability when $m \gtrsim S\log(N \cdot N \cdot L) \ll (N \cdot N \cdot L)$. In this regard, the underlying data cube is reconstructed as

$$\tilde{\boldsymbol{f}} = \boldsymbol{\Psi}\left(\underset{\boldsymbol{\theta}}{\operatorname{argmin}} ||\mathbf{y} - \mathbf{H}\boldsymbol{\Psi}\boldsymbol{\theta}||_2 + \tau||\boldsymbol{\theta}||_1\right), \tag{10}$$

where $\mathbf{H} = \left[(\mathbf{H}^0)^T, \ldots, (\mathbf{H}^{K-1})^T\right]^T$, $\boldsymbol{\theta}$ is an $S$-sparse representation of $\boldsymbol{f}$ on the basis $\boldsymbol{\Psi}$, and $\tau$ is a regularization constant [14].

## 4. SIMULATION RESULTS

In order to compare the CASSI with colored coded apertures against the traditional CASSI with photomasks, a set of compressive measurements is simulated using the forward models in Eq. (9) and Eq. (6), respectively. These measurements are constructed employing two test spectral data cubes which were acquired using a wide-band Xenon lamp as the light source, and a visible monochromator which spans the spectral range between 450nm and 650nm. The image intensity was captured using a CCD camera, exhibiting 656×492 pixels, with pixel pitch of 9.9 $\mu m$, and 8 bits of pixel depth. The resulting test data cubes $\boldsymbol{\mathcal{F}}$ have 256 × 256 pixels of spatial resolution and $L = 8$ spectral bands (Fig. 3).

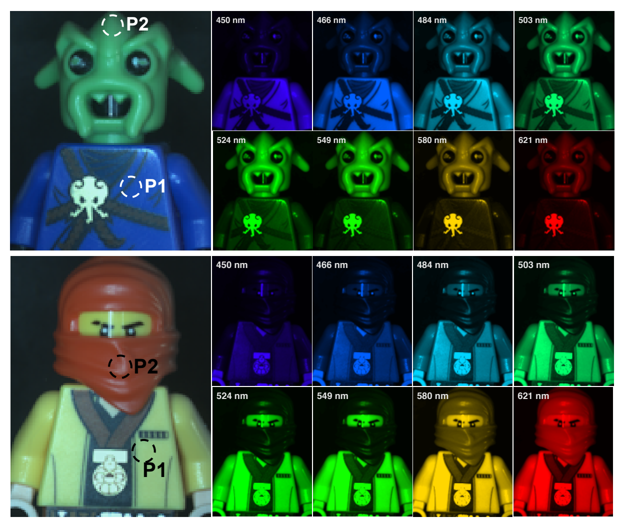


**Fig. 3**: Spectral data cubes for experimental simulations.

The photomask entries are realizations of a Bernoulli random variable, such that the number of blocking and translucent elements varies from 10% to 80%. The colored coded aperture entries are random realizations of low-pass filters, high-pass filters, and blocking elements, where the transmittance of each pattern is also varied as in the photomask case. The coding elements are designed to exhibit 256× 256 pixels of spatial resolution. The compressive sensing GPSR reconstruction algorithm [15] is used to recover the underlying data cube. The basis representation $\boldsymbol{\Psi}$ is set as the Kronecker product of two basis $\boldsymbol{\Psi} = \boldsymbol{\Psi}_1 \otimes \boldsymbol{\Psi}_2$, where $\boldsymbol{\Psi}_1$ playing the role of spatial sparsifier is the 2D-Wavelet Symmlet 8 basis and $\boldsymbol{\Psi}_2$ being the spectral sparsifier is the 1D-DCT basis. The latter selection has the advantage of a low computational cost compared to the 3D wavelet transform. Figure 4 depicts the reconstructed data cube as seen by a RGB camera when 3 snapshots are captured by both photomask-based and colored-based CASSI imagers. The improvement in the spatial quality can be observed. Figure 5 shows the PSNR of the reconstructions as function of the number of measurement shots. The gain achieved by the proposed optical architecture can also be measured by averaging the PSNR of the recovered data cubes. On the other hand, to evaluate the spectral reconstruction performance, 2 spatial points were randomly chosen, and the spectral signatures plotted in Fig. 6 when 3 snapshots were captured. Again, it can be seen how the curves using the colored coded aperture reconstructions are closer to the original. It is important to remark the impact of the transmittance in the PSNR curves at specific number of snapshots $K$. For instance, for $K = 1$ the highest PSNR is achieved when using around 40% of transmittance; for $K = 2$ it is obtained by the 30%; when $K = 3$ it is obtained by using 20%, and so on, until $K = 8$ where the best PSNR is achieved by the 10% transmittance curve. This suggests that the optimal transmittance value lies approximately around $\frac{1}{K}$.

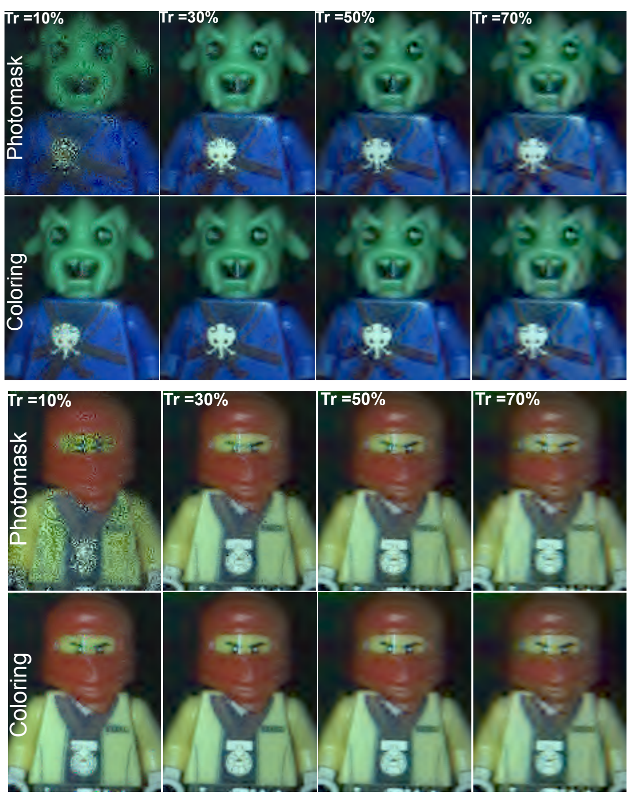


**Fig. 4**: Reconstruction of 2 different spectral data cubes mapped to a RGB profile, using $K = 3$ FPA shots and four different transmittance levels. (First and third row) Photomask approach, (Second and fourth row) Coloring approach.

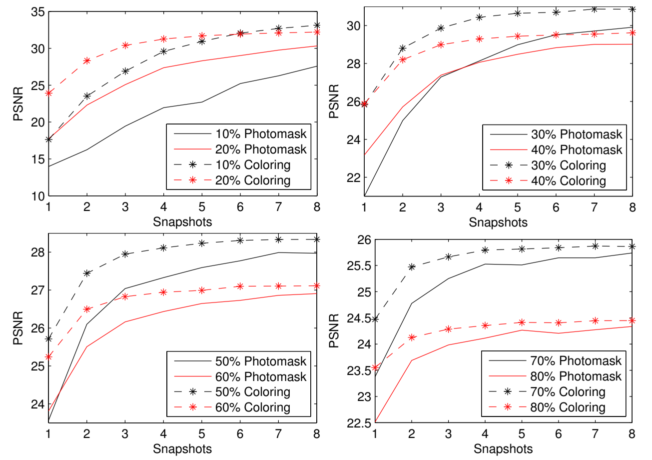


**Fig. 5**: Averaged PSNR of the reconstructed data cubes as function of the number of measurement shots. The photomask-based and the coloring-based CASSI imagers are compared at different transmittance levels.

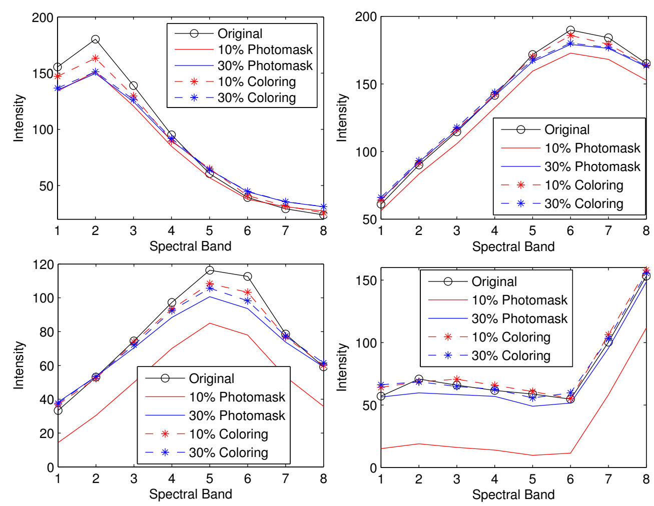


**Fig. 6**: Spectral signatures at four selected spatial points. (Top-left) P1 from database 1, (Top-right) P1 from database 2, (Bottom-left) P2 from database 1, (Bottom-right) P2 from database 2. (See Fig. 3)

## 5. CONCLUSIONS

Colored coded apertures have been successfully introduced in compressive spectral imaging systems to replace traditional block-unblock photomasks. The reconstructions with the colored CASSI attain an improvement up to 6 dB in spatial PSNR. The spectral signatures of the reconstructions get closer to the original when colored coded apertures are employed. The optimal transmittance of the colored coded apertures is inversely proportionate (approximately) to the number of measurement snapshots.

## 6. REFERENCES

[1] R.G. Sellar and G.D. Boreman, "Classification of imaging spectrometers for remote sensing applications," *Optical Engineering*, vol. 44, no. 1, pp. 013602–1, 2005.

[2] G. Nahum, "Imaging spectroscopy using tunable filters: a review," *Proc. SPIE Wavelet Applications VII*, vol. 4056, pp. 50–64, 2000.

[3] A. A. Wagadarikar, R. John, R. Willett, and D. Brady, "Single disperser design for coded aperture snapshot spectral imaging," *Appl. Opt.*, vol. 47, pp. B44–B51, 2008.

[4] G. R. Arce, D. Brady, L. Carin, H. Arguello, and D. Kittle, "An introduction to compressive coded aperture spectral imaging," *Signal Processing Magazine, IEEE*, To appear 2013.

[5] H. Arguello, H. Rueda, Y. Wu, D. W. Prather, and G. R. Arce, "Higher-order computational model for coded aperture spectral imaging," *Applied Optics*, vol. 52, no. 10, pp. D12–D21, 2013.

[6] J. M. Eichenholz and J. Dougherty, "Ultracompact Fully Integrated MegaPixel MultiSpectral Imager," *Integrated Optics: Devices, Materials, and Technologies XIII*, vol. 7218, pp. 721814–721814–10, 2009.

[7] P. A. Stupar, R. L. Borwick III, J. F. DeNatale, P. H. Kobrin, and W. J. Gunning, "Mems tunable fabry-perot filters with thick, two sided optical coatings," *Solid-State Sensors, Actuators and Microsystems Conference, 2009. TRANSDUCERS 2009. International*, pp. 1357 – 1360, June 2009.

[8] D. Hays, A. Zribi, S. Chandrasekaran, S. Goravar, S. Maity, L. R. Douglas, K. Hsu, and A. Banerjee, "A hybrid mems–fiber optic tunable fabry–perot filter," *IEEE Microelectromechanical Systems, Journal of*, vol. 19, no. 2, pp. 419 – 429, 2010.

[9] A. Brückner, *Microoptical Multi Aperture Imaging System*, Ph.D. thesis, Fraunhofer Institute for Applied Optics and Precision Engineering, Jena, 2011.

[10] S. Kim, E. Lee, M. H. Hayes, and J. Paik, "Multifocusing and depth estimation using a color shift model-based computational camera," *IEEE Trans Image Process.*, vol. 21 (9), no. 4152-4166, 2012.

[11] Y. Bando, B. Chen, and T. Nishita, "Extracting depth and matte using a color-filtered aperture," *ACM Trans. Graph.*, vol. 27, no. 5, pp. 134:1–134:9, Dec. 2008.

[12] D. Kittle, K. Choi, A. A. Wagadarikar, and D. J. Brady, "Multiframe image estimation for coded aperture snapshot spectral imagers," *Appl. Opt.*, vol. 49, no. 36, pp. 6824–6833, Dec 2010.

[13] H. Arguello and G. R. Arce, "Code aperture optimization for spectrally agile compressive imaging," *J. Opt. Soc. Am. A*, vol. 28, no. 11, pp. 2400–2413, November 2011.

[14] H. Arguello, C. Correa, and G. R. Arce., "Fast lapped block reconstructions in compressive spectral imaging.," *Applied Optics*, vol. 52, no. 10, pp. D32–D45, 2013.

[15] M. Figueiredo, R. Nowak, and S. Wright, "Gradient projection for sparse reconstruction: Application to compressed sensing and other inverse problems," *IEEE J. of Selected Topics in Signal Processing*, vol. 1, no. 4, pp. 586–597, 2007.